Resonant Raman scattering in GaAsN: Mixing, localization and band impurity formation of electronic states

Guillaume Bachelier, Adnen Mlayah, M. Cazayous, Jesse Groenen, Antoine Zwick, Hélène Carrère, Eléna Bedel-Pereira, Alexandre Arnoult, A. Rocher, Anne Ponchet

Resonant Raman scattering in GaAsN: Mixing, localization and band impurity formation of electronic states

G. Bachelier, A. Mlayah, M. Cazayous, J. Groenen, and A. Zwick
Laboratoire de Physique des Solides UMR 5477, IRSAMC,
Université P. Sabatier, 118 route de Narbonne, 31062 Toulouse Cedex 4, France

H. Carrère, E. Bedel, and A. Arnoult
Laboratoire d'Architecture et d'Analyse des Systèmes UPR 8001,
7 Av. Du Colonel Roche 31077 Toulouse, France

A. Rocher and A. Ponchet
Centre d'Elaboration de Matériaux et d'Etudes Structurales UPR 8011,
29 rue Jeanne Marvig, 31400 Toulouse, France

Raman measurements on a thick GaAsN layer and on GaAsN/GaAs quantum well structures are reported. The scattering was excited close to resonance with the N-induced E_+ transition, and detected in both Stokes and anti-Stokes regions including the low-frequency range around the Rayleigh line. A broad continuous scattering due to acoustic phonons is observed on the thick GaAsN layer. Calculations of the Raman efficiency showed that localization and mixing of the resonant electronic states well account for the measured spectral lineshapes. The localization length around a single nitrogen impurity is estimated and the band impurity formation discussed. Periodic oscillations of the scattered intensity are clearly observed on the quantum well structures. They are analyzed in terms of Raman interference effects due to spatial coherence of the resonant electronic states. We found that layering of the electronic density along the growth axis well accounts for the observed oscillations period, spectral envelope and interference contrast. The experimental data and the calculations support the formation of an impurity band.

PACS numbers: 78.30.-j, 63.20.Kr, 81.07.Ta, 81.15.Hi

I. INTRODUCTION

The substitution of only 1% As atoms by N atoms in GaAs has important impacts on the electronic and optical properties such as giant band gap bowing,[1–3] unusual pressure dependence of the band gap[4,5] and large effective masses.[6,7] Two models were proposed for the electronic structures of ternary alloys of highly mismatched binary semiconductors (e.g. GaN/GaP, GaN/GaAs, GaN/InAs). One is the band anti-crossing model (BAC), proposed by Shan *et al.*,[4,8,9] in which the electronic state of the isovalent impurity interacts strongly with the lowest conduction band states of the host material. The energies of the coupled electronic subbands, calculated using the BAC model, are in good agreement with the spectral features labelled E_- and E_+ revealed by photoreflectance (PR)[3,4] and photo-luminescence (PL)[5] measurements; the coupling strength was however used as an adjustable parameter. The BAC model is a phenomenological model since neither the origin of coupling nor the localization of the electronic states were considered explicitly. On the other hand Bellaiche *et al.*,[10] Mattila *et al.*[11] and Kent *et al.*[12,13] reported calculations of the GaAsN and GaPN electronic structure using a pseudopotential supercell technique. The composition and pressure dependence of the lowest conduction band states were studied theoretically. It was shown that E_- and E_+ are due to transitions from the valence band maximum (VBM) to conduction states involving a strongly localized nitrogen state a_1(N) mixed with host crystal states $a_1(\Gamma)$, $a_1(L)$ and $a_1(X)$ arising from the Γ, L and X valleys of the Brillouin zone. This approach well accounts for the PL and PR data as the BAC model. But in addition to the transition energies, mixing and localization of the electronic states come out as results of the calculations.[11–13]

The aim of this work is to show that mixing and localization can be addressed directly using resonant Raman scattering by acoustic phonons. Indeed, THz acoustic phonons revealed by Raman scattering have been successfully used as probes of the electronic wavefunction localization and correlation in quantum wells[14–16] and quantum dots nanostructures[17,18] . In these systems, quantum confinement and artificial, as well as spontaneous, ordering are responsible for the spatial localization and coherence of the electronic density. In GaAsN, the localization of the electronic density around the nitrogen impurity originates in the large difference between the covalent radius of N (0.075 nm) and As (0.125 nm).

In this work we estimate the localization length and degree of mixing of the resonantly excited electronic states using Raman scattering by acoustic phonons. The results

are compared to calculations performed using the pseudo-potential super-cell approach[11–13] and the large scale local density approximation.[19] Moreover, the band impurity formation is adressed using interference Raman effects generated in GaAsN/GaAs multilayers. It is worthmentioning that, among the published Raman works on GaAsN,[20–29] only few were devoted to acoustic phonons scattering.[22,29] In addition only thick GaAsN layers were studied up to now. Interference Raman effects similar to those already observed on QD layers[17,18] are here reported for the GaAsN/GaAs quantum well structures.

II. EXPERIMENTS

A 1 μm thick GaAsN layer and three GaAsN/GaAs quantum well structures were grown by molecular beam epitaxy (MBE) on (100) GaAs. The MBE chamber is equipped with a HD25R Oxford RF plasma cell, which provides reactive N species. Ultra-pure N_2 was obtained from 6N nitrogen flowing through a heating getter filter to remove O_2, H_2O, CO, CO_2 and other impurities. The growth temperatures were 580°C and 470°C for the GaAs buffer layer and for the GaAsN layer, respectively. Additional details of the growth conditions can be found elsewhere.[30]

The nitrogen concentration was determined using secondary ion mass spectroscopy (SIMS); a GaAsN layer previously characterized by X-Ray diffraction was used as a reference. Cs^+ primary ions and CsM^+ positive secondary ions configuration was used in order to provide a quantitative analysis of nitrogen content up to few percents.

Figure 1 shows transmission electron microscopy (TEM) image of the quantum well structures. Each structure consists of five GaAsN layers separated by GaAs spacers. The thickness of the GaAsN layers is around 9 nm for all structures whereas the barrier thickness is 12 nm, 24 nm or 39 nm. The GaAs top layer has the same thickness as the GaAs barriers.

For each structure the incorporation profiles of the nitrogen, along the growth direction and in the plane of the GaAsN layers, were measured using a quantitative analysis of the TEM image contrast. Typical profiles are shown in Fig. 1. For samples A and B, the nitrogen distribution inside the quantum wells is rather homogeneous. Whereas, for sample C, it is clearly non uniform. This is due to different growth conditions: the GaAs, grown before the GaAsN layers, once the plasma was ignited and the shutters still closed, was 4 nm thick for sample C and 1 nm for samples A and B, explaining why the GaAsN layers are thicker for this sample. Moreover, the plasma ignition duration may have been longer than for the other samples. Also, a lower substrate temperature (during the plasma ignition) may enhance the nitrogen deposition on the surface.

The Raman measurements were performed at liquid nitrogen temperature. The scattering was excited using

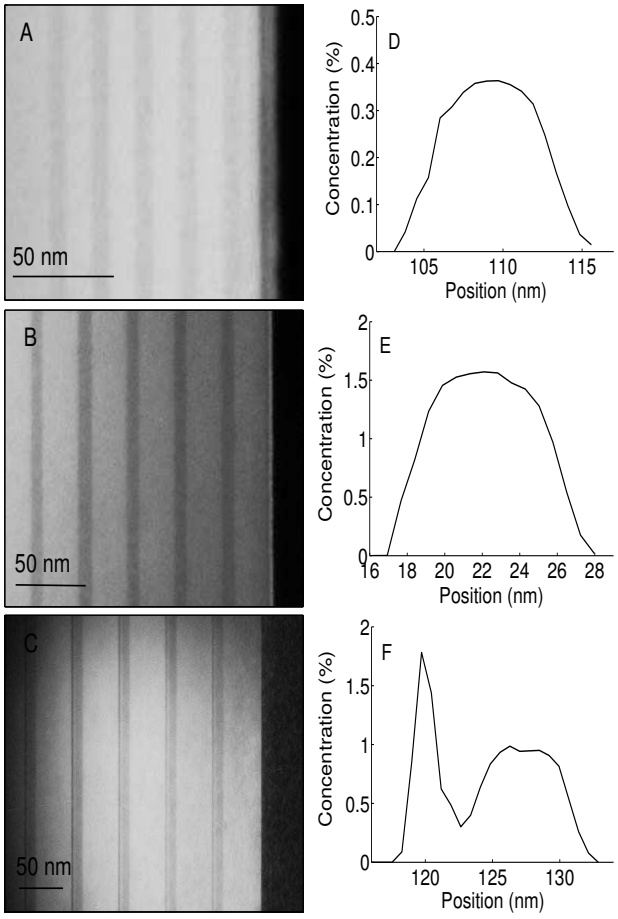

FIG. 1: TEM images of samples A, B and C. The nitrogen incorporation profiles along the growth direction were obtained by a quantitative analysis of the TEM image contrast (spectra D, E and F).

the red and yellow lines of a Kr laser. The scattered light was dispersed using a triple T800 Coderg spectrometer and detected with a single channel GaAs photo-cathode.

III. RESULTS AND DISCUSSION

Figure 2 presents Stokes and anti-Stokes Raman spectra from the thick $GaAs_{1-x}N_x$ layer with $x_{SIMS} = 0.8\%$. First and second order scattering by zone center transverse TO_Γ and longitudinal LO_Γ optical phonons of GaAs are observed. Scattering by the local vibrational mode (LVM) of isolated GaN bonds is also visible around 470 cm^{-1}. The dependence of the frequency and intensity of the TO_Γ, LO_Γ and LVM lines, on the nitrogen concentration, has been already studied in Refs. 21,23,25. In particular, Prokofyeva *et al.*[21] and Wagner *et al.*[23] showed that calibration of the frequency shift of the LO_Γ and LVM lines gives a reliable, rapid and non destructive method for determining the nitrogen content. Using the linear variations, as proposed by Prokofyeva *et al.*,[21] and the measured frequency shifts, we obtain x_{LO}=(0.8% ±

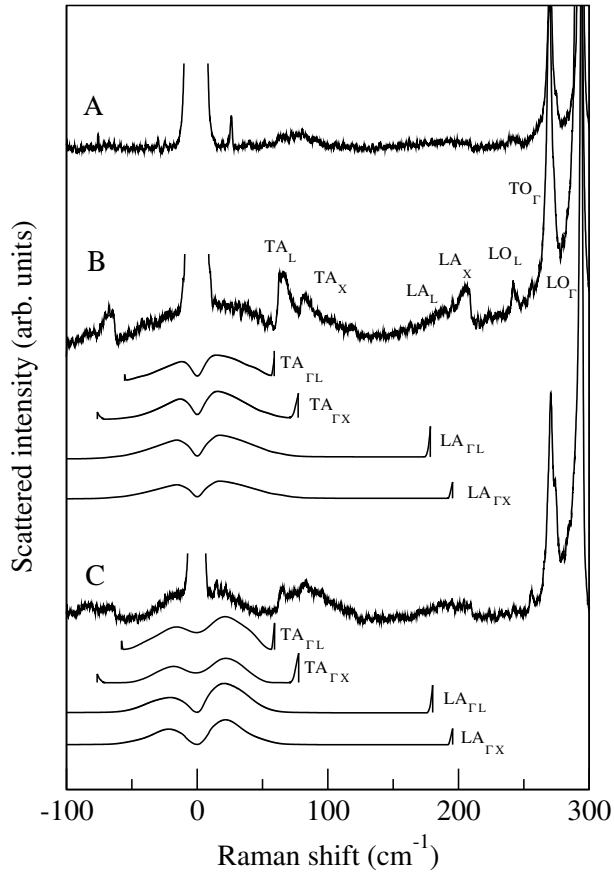

FIG. 2: Resonant Raman spectra from the 1 μm thick $GaAs_{1-x}N_x$ layer for excitation at 1.83 eV (A), 1.91 eV (B) and 1.96 eV (C). The nitrogen composition is $x_{SIMS} = 0.8\%$. Scaling factors were used in order to enable observation of the changes in the spectra. Calculated spectra show the activation of TA and LA phonons, in the Δ and Λ directions, due to wavefunction localization of the resonant state.

0.1%) and x_{LVM}= (0.9% $\pm$ 0.1%) in good agreement with $x_{SIMS} = 0.8\%$.

The spectra in Fig. 2 were excited close to resonance with the upper energy transition labeled E_+ and associated with the nitrogen impurity. According to the electro-reflectance data of Perkins *et al.*[3] we estimate E_+ around 1.86 eV (at liquid nitrogen temperature). As shown in Fig. 2, resonance occurs for excitation at 1.91 eV (647.1 nm) : first and second order scattering by the GaAs zone center phonons TO_Γ and LO_Γ and by the GaN LVM strongly come out for excitation at 1.91 eV and vanish for higher (1.96 eV) and lower (1.83 eV) energy.

In addition, spectral features due to first order scattering by zone edge acoustic (TA_X, LA_X, TA_L, TA_L) and optical phonons (LO_L, TO_X) clearly come out for resonant excitation. Such scattering has been already observed by Cheong *et al.*[22] It is normally forbidden by the wave-vector conservation rule. Indeed, as far as the wave-vector is a good quantum number, only zone-center phonon modes with wavevector $\mathbf{q}=(\mathbf{k_i} - \mathbf{k_d}) \sim 0$ can be detected ($\mathbf{k_i}$ and $\mathbf{k_d}$ being the wavevectors of the incident and scattered light, respectively). As a matter of fact, under excitation at 1.91 eV the Raman data from a GaAs reference sample showed no evidence for first order scattering by zone-edge phonons. Instead, second order scattering by zone edge TA_L phonons is allowed and could be observed because of resonance with the indirect transition from the VBM to the conduction L point.

A. Wavefunction localization

As already noted by Cheong *et al.*,[22] the observation of first order scattering by zone edge phonons is the signature of spatial localization of the resonant electronic states. Indeed, the Raman scattering is not a direct interaction between light and vibrations. It occurs via excitation and relaxation of electronic states. When these intermediate states become localized on a length scale ℓ, the wave-vector conservation rule breaks down, and phonons with wave-vectors of the order of π/ℓ can be excited. It is the spatial distribution of the electronic density that determines the spectral shape of the Raman scattering. In the frequency range of optical phonons, localization of the resonant electronic states lead only to asymmetric broadening of the Raman lines,[22] because optical phonons have relatively small frequency dispersion. In addition, their $1/q$ coupling to the electrons via Fröhlich interaction supports the Brillouin zone centre.

The frequency dispersion of acoustic phonons is quasi-linear over a wide range of the Brillouin zone. Their interaction with electrons, via deformation potential, increases as q. So, one can look to the spectral distribution of the low-frequency Raman scattering as the image of the electronic density distribution in the reciprocal space.[16–18] Conversely, one can extract the electronic density correlation function in real space from the acoustic phonon Raman spectra, allowing efficient comparison with band structure calculations.

Calculations of the GaAsN electronic structure have been performed by Mattila *et al.*[11] and Kent *et al.*[12,13] using a pseudo-potential super-cell technique. It was shown that E_+ and E_- are due to transitions from the VBM to conductions states consisting of mixed nitrogen impurity state a_1(N) and host states $a_1(\Gamma)$, $a_1(L)$ and $a_1(X)$ associated with the centre Γ and edge (L, X) points of the GaAs Brillouin zone. The degree of localization and mixing of these so-called perturbed host states (PHS) depend on the nitrogen content : In the dilute impurity limit, E_+ involves a strongly localized nitrogen a_1(N) state of which energy is inside the GaAs conduction band; this state acquires Γ and L characters and shifts to higher energy with increasing nitrogen content; it is then labeled $a_1(2)$.

For the nitrogen composition studied in Fig. 2 (x_{SIMS}=0.8%) the percentage of Γ and L components is 30% and 61%, respectively. These values were calcu-

lated by Mattila *et al.*[11] using a spectral projection of the alloy states on the GaAs Bloch states.[31] The probability for direct optical transitions from the VBM to the conduction band is proportional to the Γ component of the final state.[4] For the E_+ transition, the conduction states retain around 30% of Γ component, explaining the enhancement of the Raman efficiency at resonance with E_+ (Fig. 2). Moreover, 200 meV above $a_1(2)$ there is another mixed state labeled $a_1(3)$[12,13,19] which should also contribute to resonance. In fact, $a_1(3)$ has majority of X component (93%) and only 3% of Γ component[12] at nitrogen concentration x = 0.8%. Therefore, contribution to the resonance of the Raman scattering should be very weak in comparison with that of $a_1(2)$.

In Fig. 2 are presented Raman spectra calculated assuming wave-function localization of the resonant electronic states and interaction with acoustic phonons via deformation potential mechanism.[32] Since we are interested in the activation of all acoustic modes, including zone-edge modes, we used a polynomial fit to the measured dispersion curves,[33] rather than the linear dispersion, valid only for long-wavelength modes. Moreover, we neglected possible localization of acoustic vibrations due to N-induced disorder effects. Because of three-dimensional localization of the electronic wave-functions all orientations of phonon wave-vectors have to be taken into account. However, since mixing of electronic states involves mainly Γ, L and X states, we have considered only the [100] and [111] crystallographic directions.

We used a Gaussian wave-function centred on the nitrogen impurity for the localized electronic state; the localization length ℓ is defined as the half width at half maximum of the electronic density distribution. Actually, the calculated wave-function[13] showed a more rapid decay of the electronic density around the nitrogen impurity. We did not take into account explicitly the mixing between Γ, L and X states (except the zone-edge Fourier components of the Gaussian wave-function). In that way, one can appreciate the amount of zone-edge components (i.e. mixing) to be added to the Gaussian wave-function in order to fit the experimental spectra (Fig. 2).

Moreover, since a large number of nitrogen atoms are excited by the laser spot, we considered the scattering due to an ensemble of spatially distributed localized states. We assumed a random distribution. Such assumption should be reconsidered in the case of the quaternary alloy GaInAsN where short range order effects lead to formation of InN and GaAs bonds preferentially.[34] The ensemble wave-function is constructed simply by a coherent superposition of localized states; the average distance d between neighbouring impurities is around 1.6 nm for x = 0.8%. Hence, the electronic density could be either strongly localized with randomly distributed local maxima or totally uniform depending on the ratio ℓ/d.

The comparison between calculated and measured low-frequency Raman (Fig. 2) spectra shows that: First, the broad continuous scattering around the Rayleigh peak, and the lines due to zone edge acoustic phonons, are both due to the activation of TA and LA acoustic phonons. The very low-frequency range (-50 cm^{-1} to 50 cm^{-1}) corresponds to quasi-linear dispersion of the acoustic modes. Whereas the lines are due to nearly flat dispersion close to the Brillouin zone edges.

Second, the low frequency scattering is activated because of spatial localization of the resonant electronic states. The localization lenghts ℓ = 1.25 nm and 1.7 nm were used in the calculations for excitation at 1.91 eV and 1.83 eV, respectively. These values give a good agreement between calculated and measured spectral extent and line-shape of the low-frequency scattering (Fig. 2). Different conduction states are probed when changing the excitation energy. Our results indicate that the localization length increases when electronic states closer to the CBM are selected. This is consistent with the calculations of Kent *et al.*[12] who showed that above the limit of amalgamation between the nitrogen cluster states and perturbated host states (x ≥ 0.6%), there is a continuum of quasi-localized states within 0.4 eV above the CBM; the states close to the CBM are delocalized because of their large Γ component, whereas those around CBM = +0.4 eV exhibit localization. Indeed, according to Kent *et al.*[12] and Wang *et al.*[19] nearly 80% of the electronic density is inside a sphere of 2 nm diameter and centered at the N-impurity. Form our estimate of the localization length ℓ this percentage is 70%.

Third, TA_X, LA_X, TA_L, and TA_L lines come out strongly in the measured spectra in comparison with the calculations (spectrum B of Fig. 2): their intensity is underestimated with respect to the intensity of the broadband scattering. This is certainly due to the lack of zone edges components of the localized electronic state. As mentioned above, we used a Gaussian wave-function and hence mixing was not taken into account. The comparison with the experimental data (spectrum excited at 1.91 eV) indicates that mixing of Γ, L and X states is indeed relevant as already pointed out by Cheong *et al.*[22]. Notice that the spectrum measured at 1.83 eV compares rather well with the calculated spectra: zone edge features and broadband scattering have similar intensities. This means that the electronic conduction states selected by excitation at 1.83 eV have majority of Γ component. This is consistent with the larger localization length 1.7 nm (instead of 1.25 nm for excitation at 1.91 eV).

B. Impurity band formation

It is very interesting to compare the localization length ℓ of the electronic state around a single nitrogen impurity and the average distance d (1.6 nm) between nearest neighbourg impurities: our estimations show that $\ell \approx d$ and this indicates formation of a band impurity due to overlapping of $a_1(2)$ perturbed host states (at nitrogen content x = 0.8%). The calculations based on the pseudo-

potential method showed no evidence for the formation of an impurity band of cluster states (CS). These states are located in the band gap and are strongly localized explaining the weak CS-CS interaction and the absence of an impurity band[12]. In comparison of the CS, the PHS are less localized states and their wave-function spread over distance which could be comparable to the average separation between impurities.[12,13,19] In our calculations of the Raman spectra, the band impurity formation was not taken into account explicitly since interaction between quasi-localized $a_1(2)$ states was ignored. However, we used an ensemble wave-function which is one of the band impurity eigen-states [i.e. the one with no dephasing between the distributed $a_1(2)$ states]. In that sense, the present model for resonant Raman scattering is more realistic that the one in which only a single (average) $a_1(2)$ state is taken into account.[29] Further evidence for the formation of an impurity band is given by the interference Raman effects.

Raman scattering by acoustic vibrations is a spatially coherent process, and this leads to interference effects in the Raman efficiency: the emission and absorption rates of a given vibrational mode could be either enhanced or inhibited depending on the spatial distribution of the resonantly excited electronic density. As already shown for quantum wells[14–16] and quantum dot multi-layers,[17,18] strong oscillations of the Raman spectra could be observed in the acoustic phonons frequency range. The intensity maxima correspond to bright acoustic fringes and the minima to dark fringes. The inter-fringe, the interference contrast and the spectral envelop of the oscillations are determined by the electronic density distribution in the sample.

Figure 3 shows low-frequency Raman spectra measured from the three GaAsN/GaAs multiple quantum well structures. As mentioned in section II, the nitrogen concentration could be slightly different from sample to sample and also in comparison with the measured value for the 1 μm thick GaAsN layer. For sample C, it is clearly non uniform: strong variations are observed along the growth axis. Hence, the energy of the E_+ transition could depend on the sample. Therefore, the enhancement factor of the Raman scattering is not exactly the same for all samples since we used the same excitation energy (1.91 eV). This should also lead to selection of slightly different electronic densities. Though the output wavelength of the laser cannot be adjusted continuously, the excitation is still close to resonance with the E_+ transition for all samples.

Periodic oscillations of the low-frequency Raman spectra are clearly observed for samples A and B (Fig. 3). They originate from the interference between the Raman scattering amplitudes associated with each GaAsN quantum well. Their period is determined by the longitudinal sound velocity and by the separation between quantum wells. Their relative intensities (spectral envelop) is a form factor given by the Fourier transform of the electronic density distribution in each quantum well. The interference contrast is directly connected to the interlayer correlation of the electronic density.[17,18] For sample C, the oscillations are hardly observable due to very weak interference contrast.

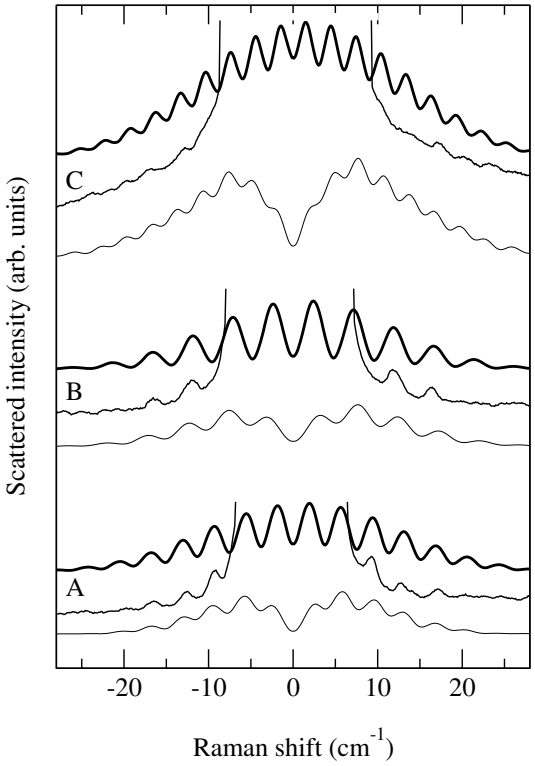

FIG. 3: Calculated and measured Raman spectra of the GaAsN/GaAs quantum well structures. Optical excitation has been performed at 1.9 eV. The thickness of the GaAs spacers is 12 nm, 24 nm and 39 nm for samples A, B and C, respectively. The spectra calculated assuming either uniform (bold line) or localized (thin line) electron density distribution (see text) in the plane of the quantum wells are shown.

Calculated Raman spectra are presented in Fig. 3. The same scattering model as the one discussed for the thick GaAsN layer has been used. The only difference with the spectra in Fig. 2 is the spatial distribution of the resonant electronic wave-function. Instead of the three-dimensional distribution of impurities, now we have layering of the wave-function along the growth direction. Moreover, since the energy of the resonant $a_1(2)$ states is above the GaAs CBM, quantum confinement effects are not expected. Then, we used an ensemble wave-function of randomly distributed nitrogen impurities in each GaAsN quantum wells with *the parameters ℓ and d obtained from the thick GaAsN layer.*

Figure 4 shows the in-plane electronic density in two of the five GaAsN/GaAs quantums wells. The parameters, such as thickness of quantum wells and distance between quantum wells, were taken from the TEM images in Fig. 1.

As one can see in Fig. 3, good agreement between calculated and measured spectra is obtained for samples A

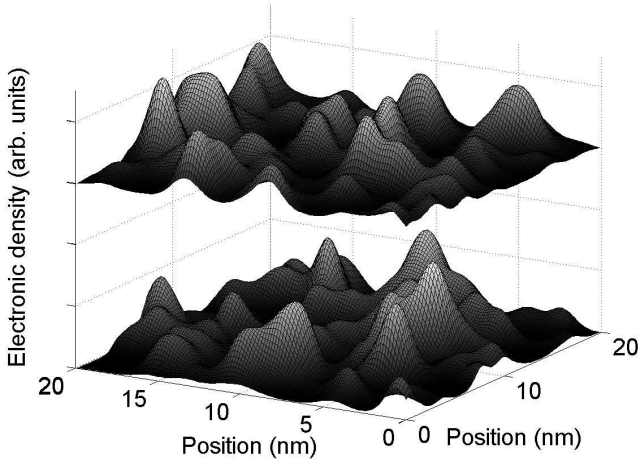

FIG. 4: In-plane electron density distribution used for the calculations of the resonant Raman spectra. They are shown only for two GaAsN/GaAs quantum wells, and were generated assuming coherent superposition of randomly distributed $a_1(2)$ states centered at the nitrogen impurities.

and B. The period and spectral envelop of the oscillations are well accounted for. As mentioned above, the interference contrast is determined by the inter-well spatial correlation of the electronic density (Fig. 4). The spectra calculated for a uniform in-plane distribution of the electronic density ($\ell \gg d$) in each quantum well are shown for comparison. In this case, the interference contrast is maximum (totally delocalized states). *The parameter l and d extracted from the thick GaAsN layer are indeed those which give the best agreement between calculated and observed interference contrast.*

Sample C, shows a much weaker interference contrast. The nitrogen distribution along the growth axis is not uniform for this sample (Fig. 1). Keeping in mind that localization and mixing of $a_1(2)$ PHS depend on the nitrogen concentration, the weaker interference contrast could be due to selection of strongly localized states ($\ell \ll d$) or to fluctuations of the nitrogen concentration in the plane of the quantum wells.

IV. CONCLUSION

Resonant Raman scattering, detected in the frequency range of acoustic phonons, reveals the spatial distribution of the excited electronic density. We have applied this approach to the study of electronic wavefunction localization in GaAsN. Our main findings can be summerized as follows. (i) By comparing calculated and measured Raman spectra we have extracted the localization length of those conduction states involved in the E_+ optical transition, namely the $a_1(2)$ states. We found a good agreement with the electronic structure predicted by the pseudo-potential supercell technique and by the large scale local density approximation. (ii) Impurity band formation has been adressed using an ensemble wavefunction for the calculations of the Raman spectra. (iii) Interference Raman effects were generated by layering the electronic density along one direction (multiple quantum wells). We have observed a strong interference contrast on two of the studied structures. This supports partial delocalization of the electronic density over many nitrogen impurities, i.e. band impurity formation of $a_1(2)$ states. The comparison between calculated and measured low-frequency Raman spectra confirm the spatial distribution of the electronic density at the studied nitrogen composition.

[1] M. Weyers, M. Sato and H. Ando, Jpn. J. Appl. Phys. **31**, L853 (1992).
[2] J. Salzman and H. Temkin, Mater. Sci. Eng. B **50**, 148 (1997).
[3] J. D. Perkins *et al.*, Phys. Rev. Lett. **82**, 3312 (1999).
[4] W. Shan *et al.*, Phys. Rev. Lett. **82**, 1221 (1999).
[5] E. D. Jones *et al.*, Phys. Rev. B **60**, 4430 (1999).
[6] Y. Zhang, A. Mascarenhas, H. P. Xin and C. W. Tu, Phys. Rev. B **61**, 7479 (2000).
[7] *et al.*, Appl. Phys. Lett. **76**, 2409 (2000).
[8] W. Shan *et al.*, Appl. Phys. Lett. **76**, 3251 (2000).
[9] W. Walukiewisz *et al.*, Phys. Rev. Lett. **85**, 1552 (2000).
[10] L.Bellaiche, Su-Huai Wei and A. Zunger, Phys. Rev. B **54**, 17568 (1996).
[11] T Mattila, Su-Huai Wei and A. Zunger, Phys. Rev. B **60**, R11245 (1999).
[12] P. R .C. Kent and A. Zunger, Phys. Rev. Lett. **86**, 2613 (2001).
[13] P. R .C. Kent and A. Zunger, Phys. Rev. B. **64**, 115208 (2001).
[14] T. Ruf in Phonon Raman scattering in Quantum wells and superlattices, **142** Springer, Berlin (1998).
[15] W. F. Sapega *et al.*, Solid. State Comm. **84** 1039 (1992).
[16] A. Mlayah *et al.*, Phys. Rev. Lett. **78**, 4119 (1997).
[17] M. Cazayous *et al.*, Phys. Rev. B **62**, 7243 (2000).
[18] M. Cazayous *et al.*, Phys. Rev. B **64**, 33306 (2001).
[19] Lin.-Wang Wang, Appl. Phys. Lett. **78**, 1565 (2001).
[20] A. M. Mintairov *et al.*, Phys. Rev. B. **56**, 15836 (1997).
[21] T. Prokofyeva *et al.*, Appl. Phys. Lett. **73**, 1409 (1998).
[22] H. M. Cheong, Y. Zhang, A. Mascarenhas and J. F. Geisz, Phys. Rev. B **61**, 13687 (2000).
[23] J. Wagner *et al.*, Appl. Phys. Lett. **77**, 3592 (2000).
[24] Y. Zhang *et al.*, Phys. Rev. B **63**, 085205 (2001).
[25] M. J. Seong, M. C. Hanna and A. Mascarenhas, Appl. Phys. Lett **79**, 3974 (2001).
[26] A. Hashimoto *et al.*, J. of Cryst. Growth **227**, 532 (2001).
[27] J. Wagner *et al.*, J. Appl. Phys. **90**, 5027 (2001).
[28] T. Geppert *et al.*, Appl. Phys. Lett. **80**, 2081 (2002).
[29] G. Bachelier *et al.*, Proceedings of the International Conference on the Physics of Semiconductors, 2002, Edin-

burgh.
[30] H. Carrère, A. Arnoult, A. Ricard, and E. Bedel-Pereira, J. Cryst. Growth **243**, 295 (2002).
[31] L. W. Wang, L. Bellaiche, S. H. Wei and A. Zunger, Phys. Rev. B **80**, 4725 (1998).
[32] B. Jusserand and M. Cardona in Light Scattering in Solids **66**, Springer, Berlin (1979).
[33] H. Bilz and W. Kreiss in Phonon Dispersion Relations in Insulators, Springer, Berlin (1979).
[34] K. Kim and A. Zunger, Phys. Rev. Lett. **86**, 2609 (2001).